Generation of tunable Fourier-transform-limited terahertz pulses in 4-*N*,*N*-dimethylamino-4′-*N*′-methyl stilbazolium tosylate crystals

Jinjun Liu and Frédéric Merkt[a)]
Laboratorium für Physikalische Chemie, ETH-Zürich, 8093 Zürich, Switzerland

(Received 1 July 2008; accepted 12 August 2008; published online 1 October 2008)

We report difference-frequency generation (DFG) of widely tunable, pulsed, Fourier-transform-limited terahertz radiation (bandwidth of ~10 MHz, peak power up to ~400 μW) from pulse-amplified near-infrared ($\lambda \sim 800$ nm) laser radiation using a crystal of the organic salt 4-*N*,*N*-dimethylamino-4′-*N*′-methyl stilbazolium tosylate (DAST) cut along the *b* axis to fulfill the phase-matching condition. The broad tunability and narrow bandwidth of the terahertz radiation generated by DFG in DAST are illustrated by a single scan of the terahertz spectrum of H_2O from 0.1 to 11 THz, and a recording of the absorption spectrum of a pure rotational transition of HF near 5 THz. © *2008 American Institute of Physics*. [DOI: 10.1063/1.2977490]

Terahertz radiation has important applications in different areas of science and technology.[1,2] Tunable, narrowband terahertz sources are of special interest in spectroscopic studies of the rotational energy level structure of light molecules, of the low-frequency vibrational structure of large molecules and weakly bound complexes, and in the identification of possible molecular carriers of astrophysical spectra.[3,4] Backward-wave-oscillator based sources and laser-based sources relying on photomixing in photoconductive materials are ideally suited to investigations in the range below 2 THz, but are difficult to operate beyond 2 THz. It is therefore particularly in this range, i.e., from 2 to 20 THz, that broadly tunable terahertz sources are currently needed.

Difference-frequency generation (DFG) from optical pump sources using nonlinear crystals represents one of the most promising methods to generate tunable terahertz radiation. The organic crystalline salt 4-*N*,*N*-dimethylamino-4′-*N*′-methyl stilbazolium tosylate (DAST), which possesses high nonlinear susceptibilities[5] compared with other materials,[6,7] represents an attractive material for terahertz generation. Terahertz radiation has been generated using DAST by optical rectification of a single femtosecond laser beam[5,8] and by DFG using two nanosecond laser beams from a dual-wavelength optical parametric oscillator (OPO) operated with either two titanium-doped sapphire (Ti:Sa) crystals[9] or two potassium titanyl phosphate (KTP) crystals.[10,11] In the latter case,[10,11] radiation could be generated throughout the terahertz region. The bandwidth of the terahertz pulses, however, was limited by the bandwidth of the OPO lasers to ~70 GHz.

Recently we have developed a technique to generate tunable Fourier-transform-limited nanosecond terahertz pulses by DFG using narrowband near-infrared (NIR) laser pulses in DAST crystals. Outputs from two narrowband ($\Delta\nu < 1$ MHz, $\lambda \sim 800$ nm) cw Ti:Sa ring lasers (Coherent, 899–29 and 899–21) were shaped into pulses of 150 ns duration using two acousto-optic modulators (AOMs) (Brimrose, GPF-1000–500–800). The first-order sideband radiation from both AOMs was coupled into a single-mode polarization-maintaining optical fiber using a 50% beam-splitter, pulse amplified in Nd:YAG (neodymium-doped yttrium aluminum garnet)-pumped Ti:Sa crystals,[12] and used as the optical source to pump an as-grown (*c*-cut) DAST crystal (Rainbow Photonics) in a collinear, normal-incident configuration with the polarizations of both frequency components parallel to the *a* axis of the crystal, making use of the χ_{111} component of the nonlinear susceptibility tensor. NIR pulse energies up to ~40 mJ could be generated from the Ti:Sa amplifier. When the crystal was pumped with ~10 kW NIR peak power, ~10 μW THz peak power was measured up to 330 GHz, limited by the spectral range of the detection system [submillimeter-wave mixer[13] and spectrum analyzer (Rohde & Schwarz, FSEK30)]. The maximal terahertz peak power was limited by the damage threshold of the DAST crystal, which was measured to be ~3 MW/cm^2 for 150 ns long laser pulses at a wavelength of 800 nm. The frequency of the first ring laser (899–29) was tuned and calibrated with the absorption spectrum of molecular iodine and a confocal

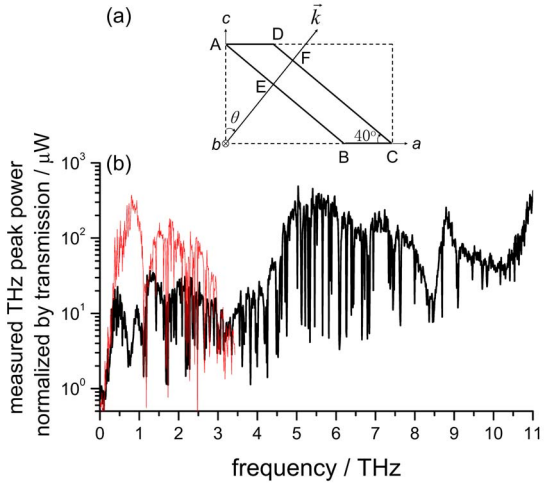

FIG. 1. (Color online) (a) DAST crystal cut for phase-matched generation of terahertz radiation by DFG using NIR radiation with wavelength around 800 nm. Note that the small deviation from perpendicularity of the *a* and *c* axes with respect to the *b* axis, 5.4° and 3.2°, respectively (Ref. 18), is neglected in the drawing of the figure. (b) Terahertz peak power generated by DFG in the cut DAST crystal using normal-incident NIR pump beams (θ=40°) with the polarizations perpendicular to the *b* axis (narrow solid line), or parallel to the *b* axis (bold solid line).

a)Electronic addresses: feme@xuv.phys.chem.ethz.ch.

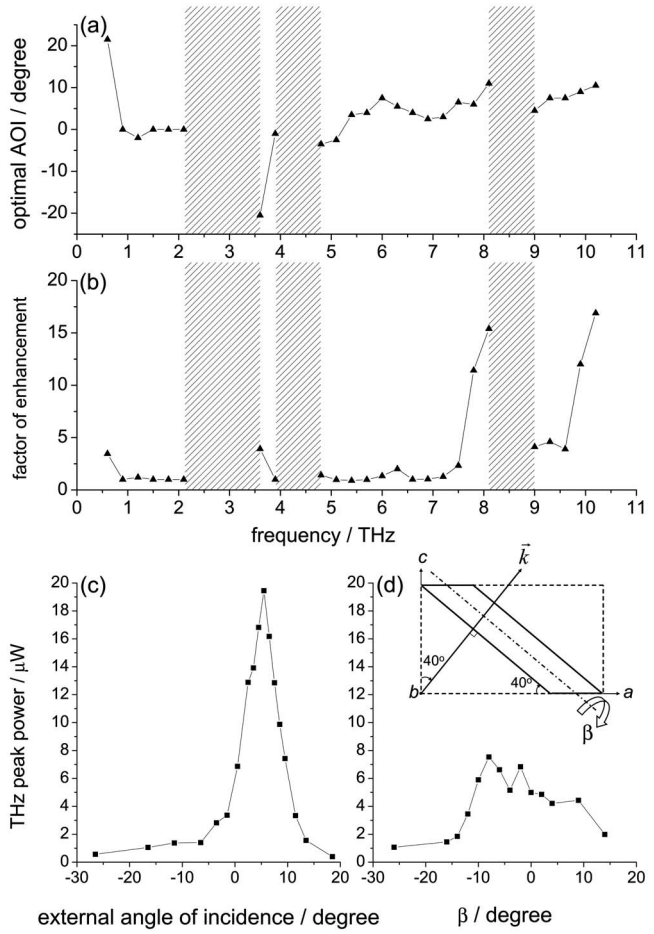

FIG. 2. (a) Optimal angle of incidence for terahertz generation by DFG in the DAST crystal using NIR laser radiation ($\lambda \sim 800$ nm) polarized parallel to the *b* axis. A positive (negative) angle refers to NIR pump beams incident from the *c* axis (*a* axis) side, i.e., $\theta > 40°$ ($\theta < 40°$). Shaded areas correspond to regions where no precise measurement could be made because of strong absorption by the DAST crystal. (b) Maximum enhancement achieved by tuning the crystal around the *b* axis. (c) Terahertz peak power at 7.5 THz as a function of the angle of incidence for NIR polarization vector parallel to the *b* axis and the wave vectors in the *ac* plane. (d) Terahertz peak power at 7.5 THz as a function of the angle between the NIR polarization vector and the *b* axis (β defined in the inset). The wave vectors are kept in the plane that is perpendicular to both the *ac* plane and the cut surfaces of the crystal.

Fabry-Pérot (FP) cavity with an absolute accuracy of ~150 MHz, while that of the second ring laser (899–21) remained locked to fringes of another FP cavity, which itself was locked to a polarization-stabilized He-Ne laser (SIOS Messtechnik GmbH, SL-02/1). The bandwidth of the terahertz pulses was determined to be ~10 MHz.[14]

Unfortunately, this approach is not practicable beyond 3 THz because the phase-matching condition cannot be fulfilled in this region using as-grown *c*-cut DAST crystals and 800 nm optical pump sources in a collinear, normal-incident configuration.[15] Prospective calculations indicated that this difficulty can be overcome by orienting the wave vectors in the *ac* plane and the polarizations of the NIR beams along the *b* axis.[14] The polarization vector of the terahertz radiation then lies in the *ac* plane and the DFG makes use of χ_{122}. By maximizing the coherence length we found that the phase-matching angle between the wave vectors and the *c* axis [θ in Fig. 1(a)] must be between 25° and 45° in most of the terahertz region.[14] The as-grown DAST crystal must therefore be cut to avoid total internal reflection.

The present letter describes experiments carried out with an as-grown DAST crystal that was cut to fulfill the phase-matching condition as described above [see Fig. 1(a)]. The dimensions of the cut surface are 4.3 mm long in the *b* direction and 5 mm long in the direction that is perpendicular to the *b* axis and makes an angle of 40° with the *a* axis (AB=CD=5 mm). The thickness of the cut crystal (EF) is 1.087 mm. The crystal was pumped by 150 ns long NIR pulses with ~16 kW peak power, which is about one order of magnitude lower than the damage threshold. The pump beams (~3 mm in diameter) propagated collinearly, and pumped the crystal in a normal-incident configuration with all wave vectors confined to the *ac* plane making an angle of $\theta = 40°$ with respect to the *c* axis. A 0.5 mm thick ultrahigh molecular weight (UHMW) black polyethylene plate was used to filter out the NIR radiation immediately after the crystal. The terahertz radiation was collected by two gold-coated off-axis parabolic mirrors. A 4.2 K germanium bolometer (IRLabs) was used to detect the terahertz radiation. Because of the far infrared cut-on filter of the detector (sapphire with ZnO, and 4/8 μm particle layers overlaid on the polyethylene antireflection coating) and of the vacuum window of the Dewar (white polyethylene with 4/8 μm diamond scatter), no radiation of frequencies higher than 11 THz could be detected. The terahertz peak power is displayed as a function of the frequency in Fig. 1(b). The spectrum was obtained in a single scan without adjusting the orientation of the crystal. In the frequency region below 3.2 THz, more radiation was detected when the polarization vector of the NIR beams lay in the *ac* plane, i.e., perpendicularly to the *b* axis, which makes use of χ_{111} and χ_{311} (solid line). Beyond 3.2 THz, no radiation was detected for the polarizations of the NIR beams perpendicular to the *b* axis in agreement with the predictions of Ref. 15. When the polarizations of the NIR beams were kept parallel to the *b* axis, the terahertz radiation remained detectable beyond 3.2 THz (bold solid line).

The terahertz peak power in Fig. 1(b) was determined from the output voltage of the bolometer using its specified responsivity (30 kV/W) and taking into account the absorption of the 0.5-mm-thick black polyethylene filter, which increases from 0% to about 90% from 0.1 to 11 THz, the absorption of the cut-on filter of the detector (~30%) and the absorption of the vacuum window of the Dewar (~30%). The numerous sharp dips in Fig. 1(b) are absorption lines of water vapor in the air (see below). The broader dips at 0.8, 1.1, 3.2, and 8.5 THz are attributed to absorptions by the crystal itself.

Both the solid and the bold solid lines in Fig. 1(b) show the terahertz output power in a normal-incident configuration, i.e., $\theta = 40°$. The terahertz output power, however, can be further optimized by adjusting the wave vectors in the *ac* plane, i.e., by adjusting the angle θ [see Fig. 1(a)], for different terahertz frequencies. The experimentally measured optimum values of θ obtained at several frequencies between 0.1 and 11 THz are plotted in Fig. 2(a). The corresponding maximum enhancement factors are displayed in Fig. 2(b). As an example, the tuning curve at 7.5 THz is given in Fig. 2(c). The sharp peak of the tuning curve centered at an angle of 5.5° clearly indicates the optimal phase-matching condition. The terahertz output power can also be optimized by adjusting the wave vectors in the plane that is perpendicular to

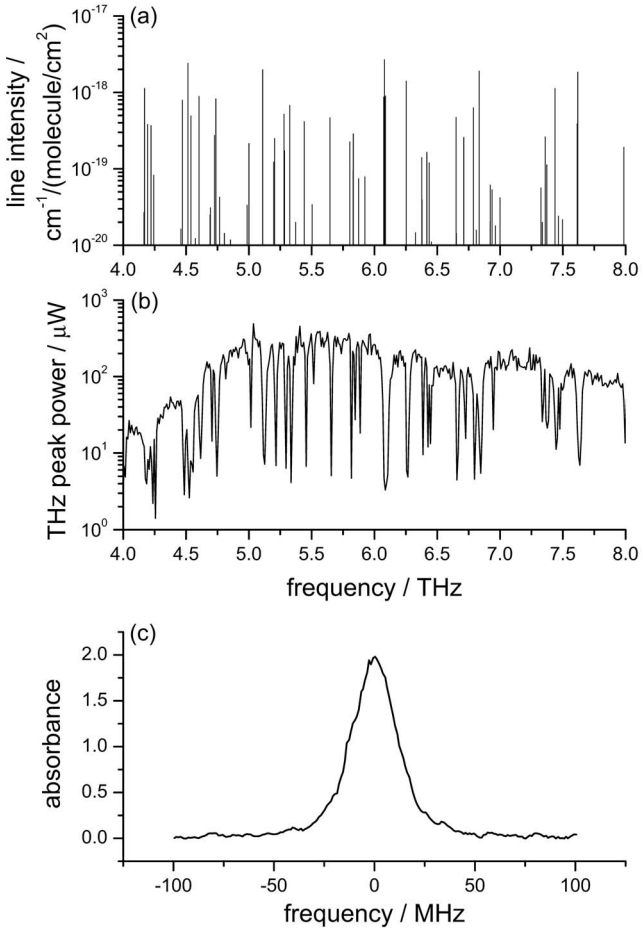

FIG. 3. (a) Water absorption lines from the HITRAN database (Ref. 16). (b) Enlarged view of the terahertz spectrum of Fig. 1(b) showing the water absorption lines in the region of 4–8 THz. (c) The absorption spectrum of a pure rotational transition of HF ($J'=4\leftarrow J''=3$). The center frequency is 4.91468257 THz (Ref. 17).

both the *ac* plane and the cut surfaces of the crystal, which causes the NIR polarization vector to slightly deviate from the *b* axis. We attribute this deviation to the angle dependence of the reflection losses and a resulting trade off between the maximum effective nonlinear susceptibility and the maximum transmission of the NIR and terahertz radiations. An example at 7.5 THz is displayed in Fig. 2(d).

Figure 1(b) demonstrates the main figure of merit of our terahertz source as a tool for future spectroscopic investigations—the wide tunability. The spectrum reveals many sharp dips caused by the absorption of water vapor in the ambient air. The water absorption lines are compared in the range of 4–8 THz with a stick spectrum generated using the HITRAN database[16] in Figs. 3(a) and 3(b). The comparison illustrates the ability of the present system to perform single broad scans over large parts of the terahertz range. The extension of the current tunable range (0.1–11 THz) to higher frequencies is expected to be straightforward because the current limitation is entirely caused by the bolometer filter. In order to demonstrate the narrow bandwidth of the terahertz source, the absorption spectrum of a pure rotational transition of HF ($J'=4\leftarrow J''=3$) was recorded in a 5-cm-long sample cell with white UHMW polyethylene windows filled with HF at a pressure lower than 0.01 mbar. The center frequency is 4.914 682 57 THz.[17] The absorption spectrum normalized by the square of the NIR laser power and converted to absorbance using Beer's law is displayed in Fig. 3(c). The full width at half maximum of the rotational line is about 25 MHz. The Doppler broadening for HF at room temperature is 13 MHz. The upper limit of the bandwidth of the terahertz source is therefore about $\sqrt{25^2-13^2}$ MHz=21 MHz. This is larger than, but comparable to, the bandwidth of ~10 MHz previously determined in the submillimeter-wave region around 300 GHz.[14] The center of the line can be determined with a precision better than 1 MHz.

We thank Professor P. Günter and Dr. A. Schneider (ETH Zurich) for useful discussions and Professor M. Quack (ETH Zurich) for lending us the bolometer. This work was supported by the Swiss National Science Foundation under Project No. 200020-116245.

[1] B. Ferguson and X.-C. Zhang, Nat. Mater. **1**, 26 (2002).
[2] F. C. De Lucia, in *Sensing with Terahertz Radiation*, edited by D. Mittleman (Springer, Berlin, 2003), pp. 39–154.
[3] D. Adam, Nature (London) **422**, 4 (2003).
[4] G. L. Pilbratt, The Institute of Space and Astronautical Science Report No. 14, 2000.
[5] A. Schneider, M. Neis, M. Stillhart, B. Ruiz, R. U. A. Khan, and P. Günter, J. Opt. Soc. Am. B **23**, 1822 (2006).
[6] S. N. Orlov and Yu. N. Polivanov, Quantum Electron. **37**, 36 (2007).
[7] S. Y. Tochitsky, C. Sung, S. E. Trubnick, C. Joshi, and K. L. Vodopyanov, J. Opt. Soc. Am. B **24**, 2509 (2007).
[8] X.-C. Zhang, X. F. Ma, Y. Jin, T.-M. Lu, E. P. Boden, P. D. Phelps, K. R. Stewart, and C. P. Yakymyshyn, Appl. Phys. Lett. **61**, 3080 (1992).
[9] K. Kawase, M. Mizuno, S. Sohma, H. Takahashi, T. Taniuchi, Y. Urata, S. Wada, H. Tashiro, and H. Ito, Opt. Lett. **24**, 1065 (1999).
[10] T. Taniuchi, S. Okada, and H. Nakanishi, J. Appl. Phys. **95**, 5984 (2004).
[11] K. Suizu, K. Miyamoto, T. Yamashita, and H. Ito, Opt. Lett. **32**, 2885 (2007).
[12] R Seiler, Th. Paul, M. Andrist, F. Merkt, Rev. Sci. Instrum. **76**, 103103 (2005).
[13] A. M. Schitov, G. Yu. Golubyatnikov, M. Yu. Tretyakov, S. A. Volokhov, and A. Walters, Int. J. Infrared Millim. Waves **21**, 1479 (2000).
[14] J. Liu, H. Schmutz, and F. Merkt (unpublished).
[15] P. Y. Han, M. Tani, F. Pan, and X.-C. Zhang, Opt. Lett. **25**, 675 (2000).
[16] L. S. Rothman, D. Jacquemart, A. Barbe, D. C. Benner, M. Birk, L. R. Brown, M. R. Carleer, C. Chackerian Jr., K. Chance, L. H. Coudert *et al.*, J. Quant. Spectrosc. Radiat. Transf. **96**, 139 (2005).
[17] I. G. Nolt, J. V. Radostitz, G. DiLonardo, K. M. Evenson, D. A. Jennings, K. R. Leopold, M. D. Vanek, L. R. Zink, A. Hinz, and K. V. Chance, J. Mol. Spectrosc. **125**, 274 (1987).
[18] G. Knöpfle, R. Schlesser, R. Ducret, and P. Günter, Nonlinear Opt. **9**, 143 (1995).